LEHIGH UNIVERSITY

INTERACTION BETWEEN PARALLEL CRACKS IN

LAYERED COMPOSITES

By

M. RATWANI

AND

G. D. GUPTA

TECHNICAL REPORT NASA TR-73-6

MARCH 1973

INTERACTION BETWEEN PARALLEL CRACKS
IN LAYERED COMPOSITES*

by
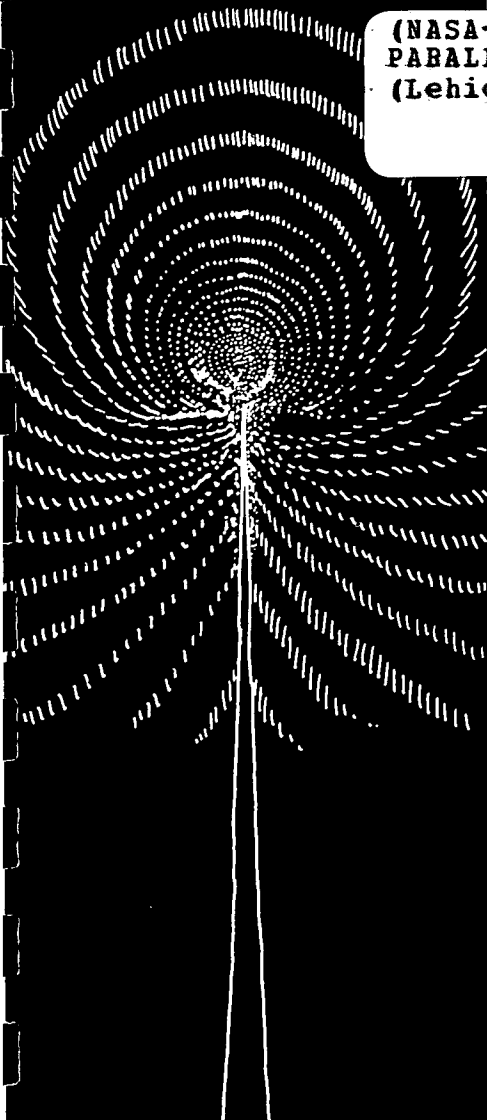
M. Ratwani and G. D. Gupta
Lehigh University, Bethlehem, Pennsylvania

ABSTRACT

The plane strain problem of a multi-layered composite with parallel cracks in considered. The main objective of this paper is to study the interaction between parallel and collinear cracks. The problem is formulated in terms of a set of simultaneous singular integral equations which are solved numerically. The effect of material properties on the interaction between cracks is also demonstrated.

INTRODUCTION

Welded and bonded structures have been observed to contain multiple cracks. The study of the interaction between such cracks has also been of considerable interest to reactor designers. The problem of a multi-layered composite containing a single crack was studied by Erdogan and Gupta [1-2]. The interaction between multiple cracks in an isotropic medium and collinear cracks in a layered composite has been considered by Ratwani [3-4].

In the present study, the analytical methods of [1-4] have been extended to treat the layered composite containing parallel and collinear cracks. In particular, the plane strain problem of an elastic layer bonded to two dissimilar half-planes is considered. The layer medium contains one or two symmetrically placed collinear flaws and one of the half-planes is assumed to have a single parallel flaw. The procedure, of course, can easily treat any composite containing n elastic layers and cracks located along m parallel planes. For the sake of simplicity, only the symmetric problem is studied here. The anti-symmetric loading case can be handled in an analogous manner.

Stress intensity factors at all the crack tips are computed. Their variation with respect to the crack locations, geometry and material of the composite are presented graphically.

FORMULATION OF THE PROBLEM

Consider the plane problem, shown in Figure 1, containing one or two collinear cracks in each plane. The cracks are assumed to be located symmetrically with respect to the y-axis. In this paper, our primary interest is in the disturbed stress state caused by the cracks. Hence, assuming that the overall stress distribution $\sigma_{ij}{}^0$ in the imperfection-free medium is known, the stress state $\sigma_{ij}{}^T$ in the cracked medium may be expressed as

$$\sigma_{ij}{}^T = \sigma_{ij}{}^0 + \sigma_{ij} \tag{1}$$

where σ_{ij} is the disturbed stress state obtained by subjecting the crack surfaces to the following tractions.

$$\sigma_{yy}{}^1(x,h) = - \sigma_{yy}{}^0(x,h) = p_2(x)$$
$$\sigma_{xy}{}^1(x,h) = - \sigma_{xy}{}^0(x,h) = p_1(x) \qquad , \qquad C<|x|<D,$$

$$\tag{2}$$

$$\sigma_{yy}{}^3(x,-h_1) = - \sigma_{yy}{}^0(x,-h_1) = q_2(x)$$
$$\sigma_{xy}{}^3(x,-h_1) = - \sigma_{xy}{}^0(x,-h_1) = q_1(x) \qquad , \qquad A<|x|<B.$$

$p_i(x)$ and $q_i(x)$ satisfy a Hölder condition in their respective ranges.

The integral transform technique, described in detail for a single crack [1] and for multiple cracks [3], is used here to formulate the problem in terms of four unknown functions defined by

$$f_1(x) = \frac{\partial}{\partial x}(u_2 - u_1), \quad f_2(x) = \frac{\partial}{\partial x}(v_2 - v_1), \quad (C < |x| < D, \ y = h),$$

$$\tag{3}$$

$$g_1(x) = \frac{\partial}{\partial x}(u_3 - u_4), \quad g_2(x) = \frac{\partial}{\partial x}(v_3 - v_4), \quad (A < |x| < B, \ y = -h_1).$$

Note that the crack surfaces are the singular surfaces across which the displacement vector suffers a discontinuity and the unknown functions define the derivatives of the crack opening displacements. For the sake of simplicity, the central plane of the elastic layer is assumed to have the cracks. The case when the crack lies at the interface between the bielastic media has been treated in detail in [2].

Following the procedure of [1] and [3], a set of simultaneous singular integral equations of the first kind is derived, expressed as follows:

$$\int_{L_1} \sum_{j=1}^{2} f_j(t)[\frac{\delta_{ij}}{t-x} + K_{ij}(x,t)]dt + \int_{L_2} \sum_{k=1}^{2} g_k(\tau) H_{ik}(x,\tau) d\tau$$

$$= \frac{1+\kappa_1}{2\mu_1} \pi p_i(x) , \qquad C < |x| < D, \ i = 1,2,$$

$$\tag{4}$$

$$\int_{L_1} \sum_{j=1}^{2} f_j(t) L_{ij}(x,t) dt + \int_{L_2} \sum_{k=1}^{2} g_k(\tau)[\frac{\delta_{ik}}{\tau-x} + M_{ik}(x,\tau)] d\tau$$

$$= \frac{1+\kappa_2}{2\mu_2} \pi q_i(x) , \qquad A < |x| < B, \ i = 1,2,$$

where $L_1 \equiv (C < |x| < D)$ and $L_2 \equiv (A < |x| < B)$, and $\kappa_i = 3 - 4\nu_i$ for plane strain and $\kappa_i = (3 - \nu_i)/(1 + \nu_i)$ for generalized plane stress. μ_i and ν_i are the shear modulii and the Poisson's ratios, for $i = 1,2$, denoting the elastic layer by the subscript 1 and the half-planes by 2. The functions K_{ij}, L_{ij}, H_{ik} and M_{ik}

-3-

are Fredholm kernels and are bounded in their respective closed intervals. The expressions for these Fredholm kernels are given as follows:

$$K_{11}(x,t) = \int_0^\infty \frac{s_1(\alpha) - 4\alpha h}{D_1(\alpha)} e^{-2\alpha h} \sin\alpha(t-x)d\alpha$$

$$K_{12}(x,t) = K_{21}(x,t) = 0$$

$$K_{22}(x,t) = \int_0^\infty \frac{s_1(\alpha) + 4\alpha h}{D_2(\alpha)} e^{-2\alpha h} \sin\alpha(t-x)d\alpha$$

$$H_{11}(x,\tau) = \frac{\mu_2}{\mu_2-\mu_1} \frac{1+\kappa_1}{2\lambda_3} \int_0^\infty [\lambda_3 s_3(\alpha) + (1 - 2\alpha h_1)s_2(\alpha)] \cdot$$
$$\frac{e^{-\alpha(h+h_1)}}{D_1(\alpha)} \sin\alpha(\tau-x)d\alpha$$

$$H_{12}(x,\tau) = \frac{\mu_2}{\mu_2-\mu_1} \frac{1+\kappa_1}{2\lambda_3} \int_0^\infty [\lambda_3 s_3(\alpha) - (1 + 2\alpha h_1)s_2(\alpha)] \cdot$$
$$\frac{e^{-\alpha(h+h_1)}}{D_1(\alpha)} \cos\alpha(\tau-x)d\alpha$$

$$H_{21}(x,\tau) = \frac{\mu_2}{\mu_2-\mu_1} \frac{1+\kappa_1}{2\lambda_3} \int_0^\infty [\lambda_3 s_5(\alpha) - (1 - 2\alpha h_1)s_4(\alpha)] \cdot$$
$$\frac{e^{-\alpha(h+h_1)}}{D_2(\alpha)} \cos\alpha(\tau-x)d\alpha$$

$$(5)$$

$$H_{22}(x,\tau) = - \frac{\mu_2}{\mu_2-\mu_1} \frac{1+\kappa_1}{2\lambda_3} \int_0^\infty [\lambda_3 s_5(\alpha) + (1 + 2\alpha h_1)s_4(\alpha)] \cdot$$
$$\frac{e^{-\alpha(h+h_1)}}{D_2(\alpha)} \sin\alpha(\tau-x)d\alpha$$

$$L_{ij}(x,t) = \frac{(\mu_2-\mu_1)^2(\lambda_1-\lambda_2)\lambda_3}{\mu_2^2(1+\kappa_1)^2} H_{ij}(x,t) , \qquad i,j = 1,2$$

$$M_{11}(x,\tau) = -\frac{1}{2} \int_0^\infty \left[\lambda_3 + s_8(\alpha) + \frac{(\lambda_1-\lambda_2)}{D_1(\alpha)D_2(\alpha)} \{ \lambda_3 s_7(\alpha) \right.$$

$$\left. + [s_7(\alpha)s_8(\alpha) - 8\alpha h(1 - 2\alpha h_1)]e^{-4\alpha h}\} \right] e^{-2\alpha h_1} \sin\alpha(\tau-x)d\alpha$$

$$M_{12}(x,\tau) = -\frac{1}{2} \int_0^\infty \left[\lambda_3 - s_6(\alpha) + \frac{(\lambda_1-\lambda_2)}{D_1(\alpha)D_2(\alpha)} \{ \lambda_3 s_7(\alpha) \right.$$

$$\left. + [16\alpha^2 h h_1 - s_6(\alpha)s_7(\alpha)]e^{-4\alpha h}\} \right] e^{-2\alpha h_1} \cos\alpha(\tau-x)d\alpha$$

$$M_{21}(x,\tau) = M_{12}(x,\tau)$$

$$M_{22}(x,\tau) = -\frac{1}{2} \int_0^\infty \left[\lambda_3 + s_9(\alpha) + \frac{(\lambda_1-\lambda_2)}{D_1(\alpha)D_2(\alpha)} \{ \lambda_3 s_7(\alpha) \right.$$

$$\left. - [s_7(\alpha)s_9(\alpha) - 8\alpha h(1 + 2\alpha h_1)]e^{-4\alpha h}\} \right] e^{-2\alpha h_1} \sin\alpha(\tau-x)d\alpha$$

where

$$D_1(\alpha) = -\lambda_2 + (4\alpha h + \lambda_1 e^{-2\alpha h})e^{-2\alpha h}$$

$$D_2(\alpha) = \lambda_2 + (4\alpha h - \lambda_1 e^{-2\alpha h})e^{-2\alpha h}$$

$$s_1(\alpha) = 1 + \lambda_1\lambda_2 + 4\alpha^2 h^2 - 2\lambda_1 e^{-2\alpha h}$$

$$s_2(\alpha) = -\lambda_2 + (1 + 2\alpha h)e^{-2\alpha h}$$

$$s_3(\alpha) = 1 - 2\alpha h - \lambda_1 e^{-2\alpha h}$$

$$s_4(\alpha) = \lambda_2 - (1 - 2\alpha h)e^{-2\alpha h} \tag{6}$$

$$s_5(\alpha) = -1 - 2\alpha h + \lambda_1 e^{-2\alpha h}$$

$$s_6(\alpha) = (1 - 4\alpha^2 h_1^2)/\lambda_3$$

$$s_7(\alpha) = -\lambda_2 + \lambda_1 e^{-4\alpha h}$$

$$s_8(\alpha) = (1 - 2\alpha h_1)^2/\lambda_3$$

$$s_9(\alpha) = (1 + 2\alpha h_1)^2/\lambda_3$$

and

$$\lambda_1 = \frac{\mu_1\kappa_2 - \mu_2\kappa_1}{\mu_2 + \mu_1\kappa_2}$$

$$\lambda_2 = \frac{\mu_1 + \mu_2\kappa_1}{\mu_1 - \mu_2} \tag{7}$$

$$\lambda_3 = \frac{\mu_2 + \mu_1\kappa_2}{\mu_2 - \mu_1} .$$

The unknown functions f_i and g_i in equations (4) have integrable singularities at the end points. Therefore, the equations (4) must be solved subject to the singlevaluedness conditions

$$\int_C^D f_i(t)dt = 0 = \int_A^B g_i(t)dt , \qquad i=1,2. \tag{8}$$

The singular integral equations (4) are solved simultaneously by using the numerical technique described in [5]. It may be noted that if one of the cracks lies on the interface, the corresponding integral equation would become that of second kind. The numerical technique to treat such equations is described in [6] and is used to solve the interface crack problems in [2]. The stress intensity factors K_I and K_{II} at all the crack tips are defined as in [1]. As an example, for the crack in medium (1) near the crack tip $x \to D$, these can be expressed as

$$K^1_I = \lim_{x \to D} \sqrt{2(x-D)} \; \sigma_{yy}^1(x,h)$$

$$K^1_{II} = \lim_{x \to D} \sqrt{2(x-D)} \; \sigma_{xy}^1(x,h) \; . \tag{9}$$

The stress intensity factors can also be expressed in terms of the unknown functions $f_i(x)$. The functions $f_i(x)$, which have integrable singularities, may be written as

$$f_i(x) = \frac{G_i(x)}{\sqrt{(D-x)(x-C)}} \; . \tag{10}$$

Equations (9) can now be written as

$$K^1_I = - \frac{2\mu_1}{1+\kappa_1} \lim_{x \to D} \sqrt{2(D-x)} \; f_2(x)$$

$$= - \frac{2\mu_1}{1+\kappa_1} \sqrt{\frac{2}{D-C}} \; G_2(D)$$

$$\tag{11}$$

$$K^1_{II} = \frac{2\mu_1}{1+\kappa_1} \lim_{x \to D} \sqrt{2(D-x)} \; f_1(x)$$

$$= \frac{2\mu_1}{1+\kappa_1} \sqrt{\frac{2}{D-C}} \; G_1(D) \; .$$

Superscripts 1 and 2 on the stress intensity factors refer to the cracks in medium 1 and 2 respectively.

DISCUSSION OF RESULTS

To demonstrate the interaction between parallel cracks, a layered composite as shown in Figure 1 is assumed to contain two parallel cracks, one in the mid-plane of the elastic layer and the other in one of the half-planes. Figures 2-9 show the variations of the four stress intensity factors (at each crack tip)

with the material and geometrical parameters entering into the problem. First an epoxy layer with elastic properties $\mu_1 = 4.5 \times 10^5$ psi, $\nu_1 = 0.35$ is sandwiched between two aluminum half-planes: $\mu_2 = 10^7$ psi and $\nu_2 = 0.3$. Since the primary objective of this work was to study the disturbance problem, the input tractions were assumed to be uniform uni-axial stresses with zero shear component, i.e., in equation (2)

$$p_1(x) = q_1(x) = 0$$

$$p_2(x) = \sigma_0 \qquad \text{or} \qquad (12)$$

$$q_2(x) = \sigma_0 \; .$$

The crack in medium 1 was loaded first and, as expected, we get negative stress intensity factors for crack 2. The results are shown in Figure 2. Figure 3 shows similar results when only the crack in medium 2 was loaded. It is clear that the results need to be superimposed if both the cracks are loaded simultaneously. In Figures 2 and 3, the stress intensity factors K^1_I, K^1_{II}, K^2_I and K^2_{II} with respect to the distance of crack 2 from the interface are shown. The two cracks have been assumed to be of equal length. We observe that the absolute magnitudes of all the K values increase as crack 2 nears the interface. The layer thickness here was assumed to be equal to the crack length. Figures 4 and 5 show similar plots for a layer of double the thickness. Notice the decrease in the interaction between the two cracks since they are farther apart now. Also, the stress intensity factors at crack 1 due to the loading at this crack increase due to increasing the layer thickness. In limit when $h \to \infty$, $K^1_I = 1.0$,

$K^1_{II} = K^2_I = K^2_{II} = 0$. This effect is depicted in Figure 6, where the stress intensity factors are plotted with respect to the layer thickness. However, a reverse effect is observed at the stress intensity factors at crack 2 due to the loading at crack 2 itself, as shown in Figure 7. K^2_I and K^2_{II} decrease as the layer thickness is increased and, in the limiting case when $h \to \infty$, these approach asymptotically to the values obtained for the problem of a bimaterial medium containing a single crack in one of the half-planes. Interaction terms, of course, vanish as $h \to \infty$. Figures 8 and 9 show the effect of the material properties of the composite constituents. Here an aluminum layer is bonded between two epoxy half-planes. Similar observations are made when the crack in medium 2 approaches the interface and when the layer thickness is increased.

As a second example, the case of the elastic layer containing two collinear cracks at the mid-plane and located symmetrically is considered. Since the problem is symmetrical, stress intensity factors at only one of the collinear cracks need be computed. In all numerical cases, the location of crack 2 and the layer thickness have been kept fixed. Again either the collinear cracks or crack 2 is loaded at a time. Variation of the mode I stress intensity factor with respect to the distance between the collinear cracks is shown in Figure 10. When these collinear cracks are far away, only a little interaction between the parallel crack is observed. Another interesting phenomenon observed is that, if the two collinear cracks are close by, i.e.,

c/a < 1.25 (see insert in Figure 10 for the notation), the un-
stable crack propagation would first take place at the inner
crack tip, thus generating a single crack in the layer. On the
contrary, if the two cracks are far apart, i.e., if c/a > 1.25,
the outer crack tips would become unstable before the inner
crack tip. Figure 11 illustrates the mode II stress intensity
factors for the same problem. When crack 2 is loaded, the
stress intensity factors K^2_I and K^2_{II} remain practically unaf-
fected due to the displacement of the collinear crack locations
(Figure 12). However, the interaction between these cracks is
quite strongly affected by the distance between the two collin-
ear cracks, as shown in Figure 13. Again, when the two cracks
come closer, K_I at both the crack tips increases monotonically,
with faster rise in the inner crack tip. K_{II} at the inner tip,
however, undergoes a maximum value and steadily decreases to a
very low value.

In conclusion, whenever there is a structure containing
multiple cracks, an analysis of the type described in this paper
is essential in order to find the critical configurations under
which the structure may be most vulnerable.

REFERENCES

1. F. Erdogan and G. Gupta, "The Stress Analysis of Multi-Layered Composites with a Flaw", International Journal of Solids Structures, Vol. 7, pp. 39-61, 1971.

2. F. Erdogan and G. D. Gupta, "Layered Composites with an Interface Flaw", International Journal of Solids Structures, Vol. 7, pp. 1089-1107, 1971.

3. M. Ratwani, "Wechselwirkung Von Rissen", Institüt für Festkörpermechanik der Fraunhofer-Gesellschaft, Freiburg, West Germany, Report 5/72.

4. M. Ratwani, "Mehrfach Rissen im Verbundmaterialen", Institüt für Festkörpermechanik der Fraunhofer-Gesellschaft, Freiburg, West Germany, Report 6/72.

5. F. Erdogan and G. D. Gupta, "On the Numerical Solution of a Singular Integral Equation", Quarterly of Applied Mathematics, pp. 525-534, 1972.

6. F. Erdogan, "Approximate Solution of Systems of Singular Integral Equations", SIAM Journal of Applied Mathematics, 17, pp. 1041-1059, 1969.
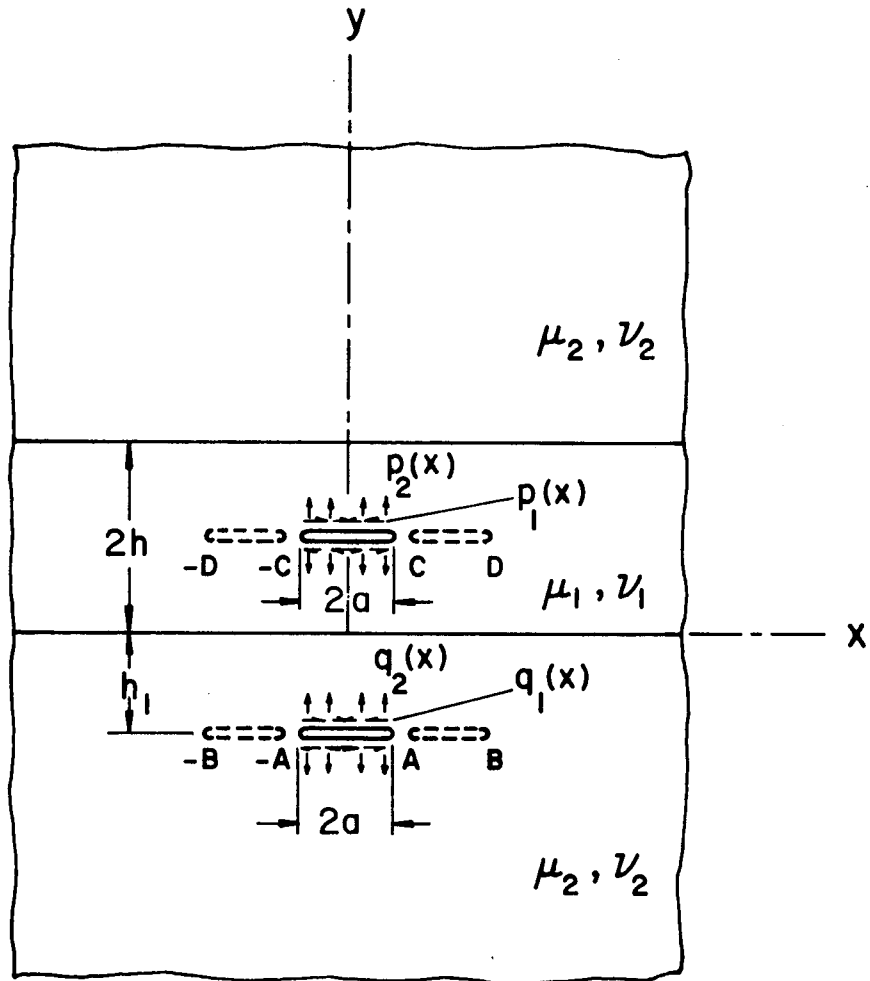
Figure 1. Geometry of the Layered Composite
with Collinear and Parallel Cracks.
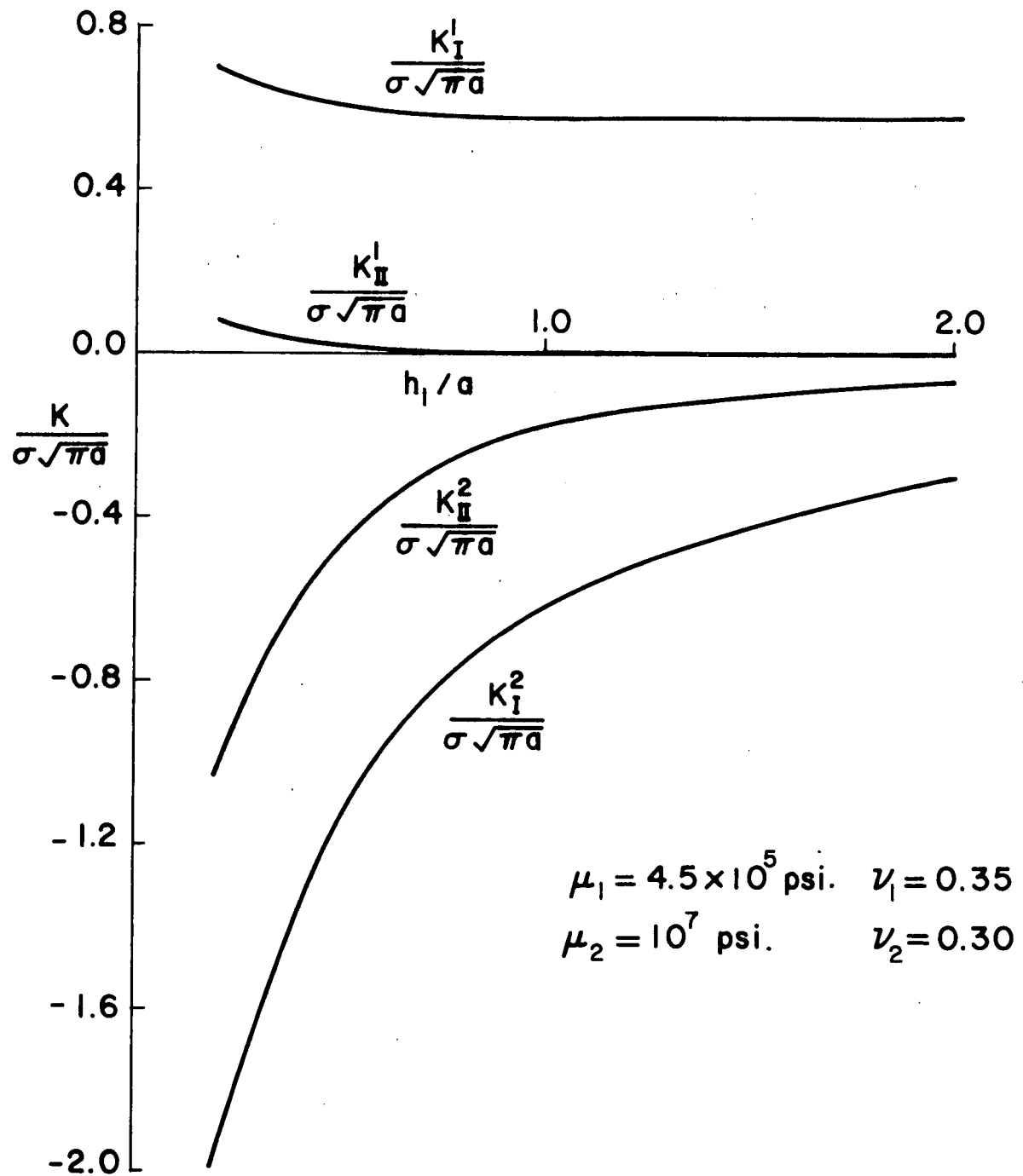
Figure 2. Stress Intensity Factors vs. h_1/a for $h/a = 1.0$,
$p_2(x) = -\sigma$ and $p_1(x) = q_1(x) = q_2(x) = 0$.
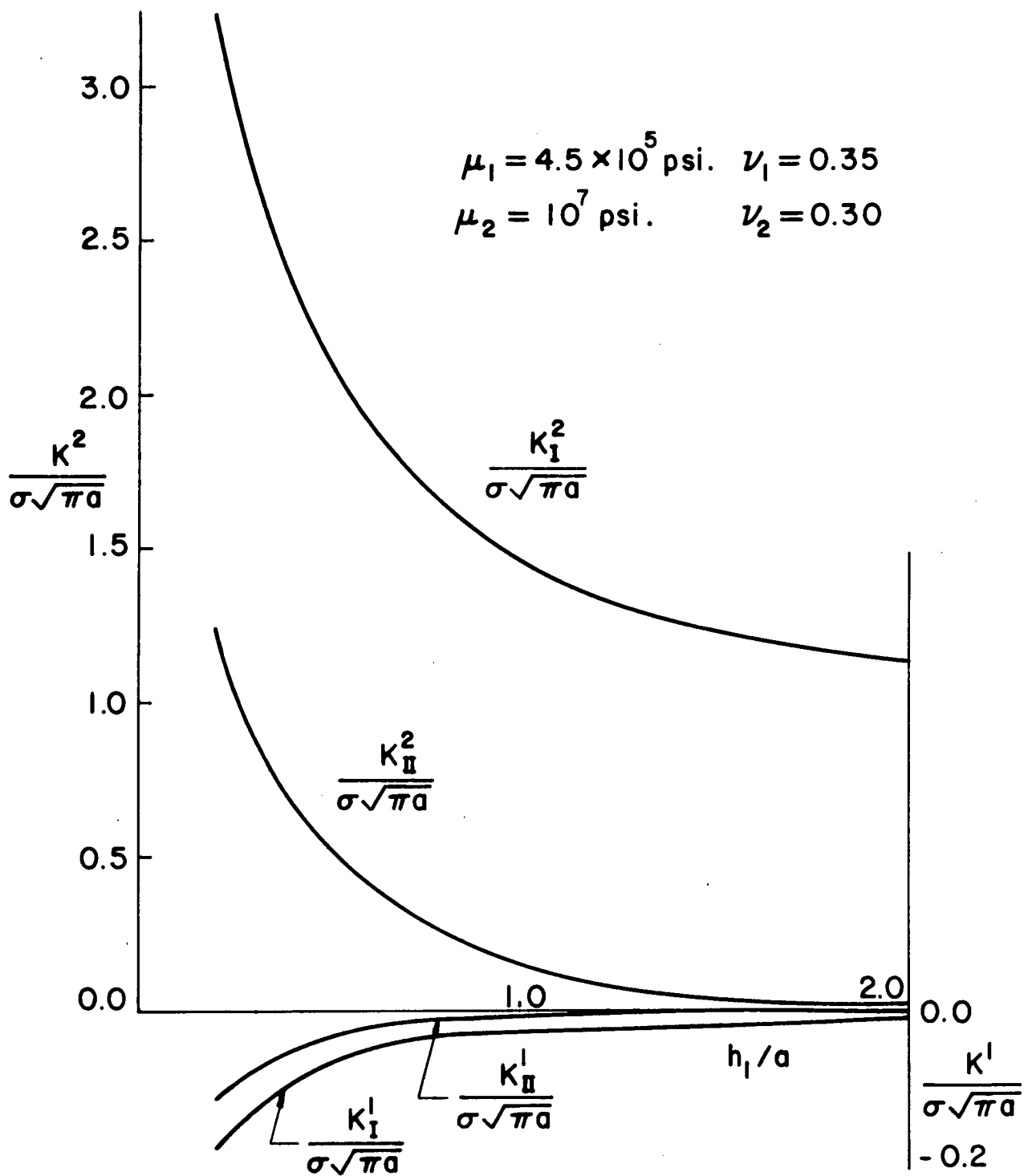
Figure 3. The Case with $q_2(x) = -\sigma$ and $p_1(x) = p_2(x) = q_1(x) = 0$.
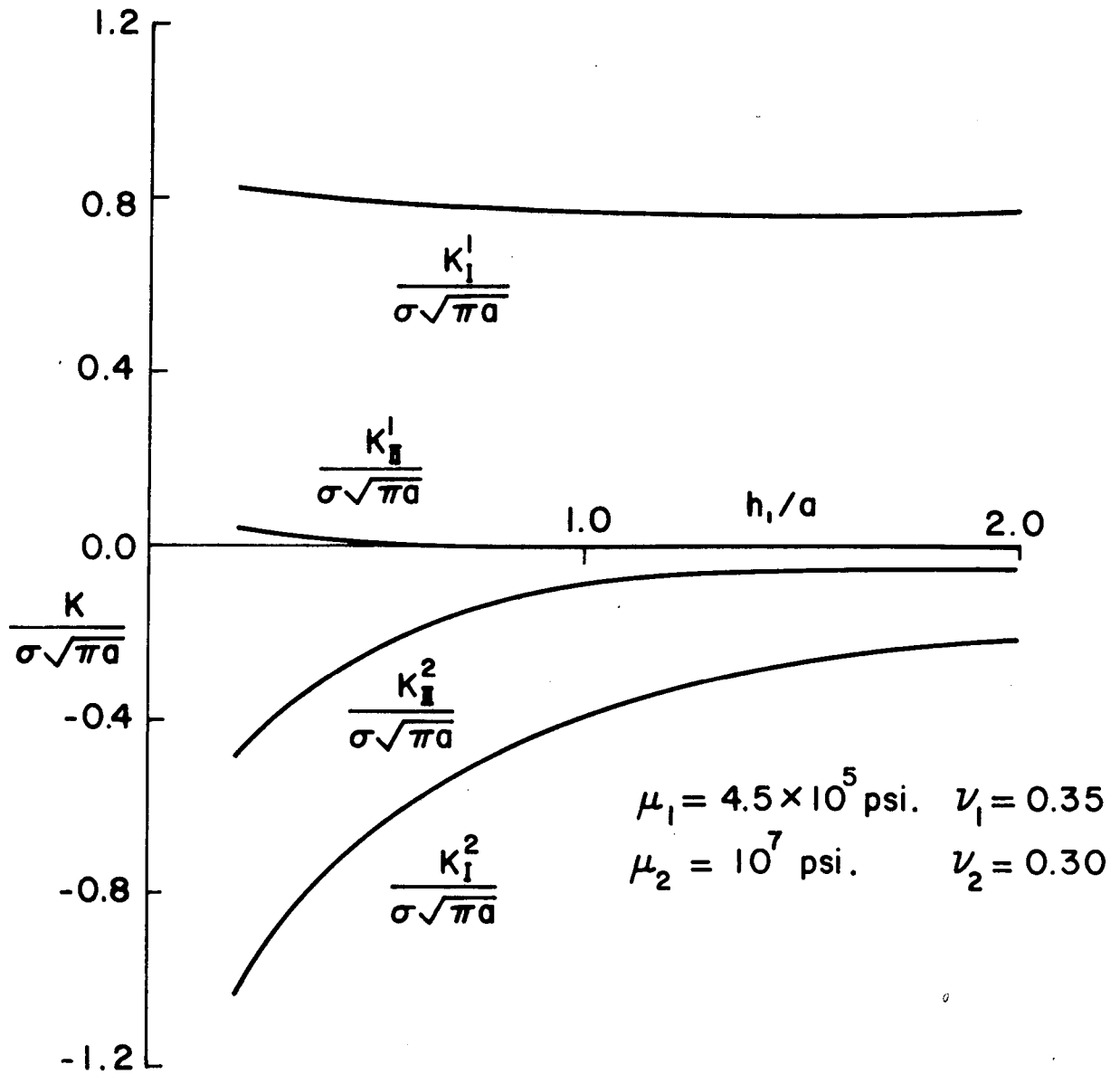
Figure 4. Stress Intensity Factors vs. h_1/a for $h/a = 2.0$, $p_2(x) = -\sigma$ and $p_1(x) = q_1(x) = q_2(x) = 0$.
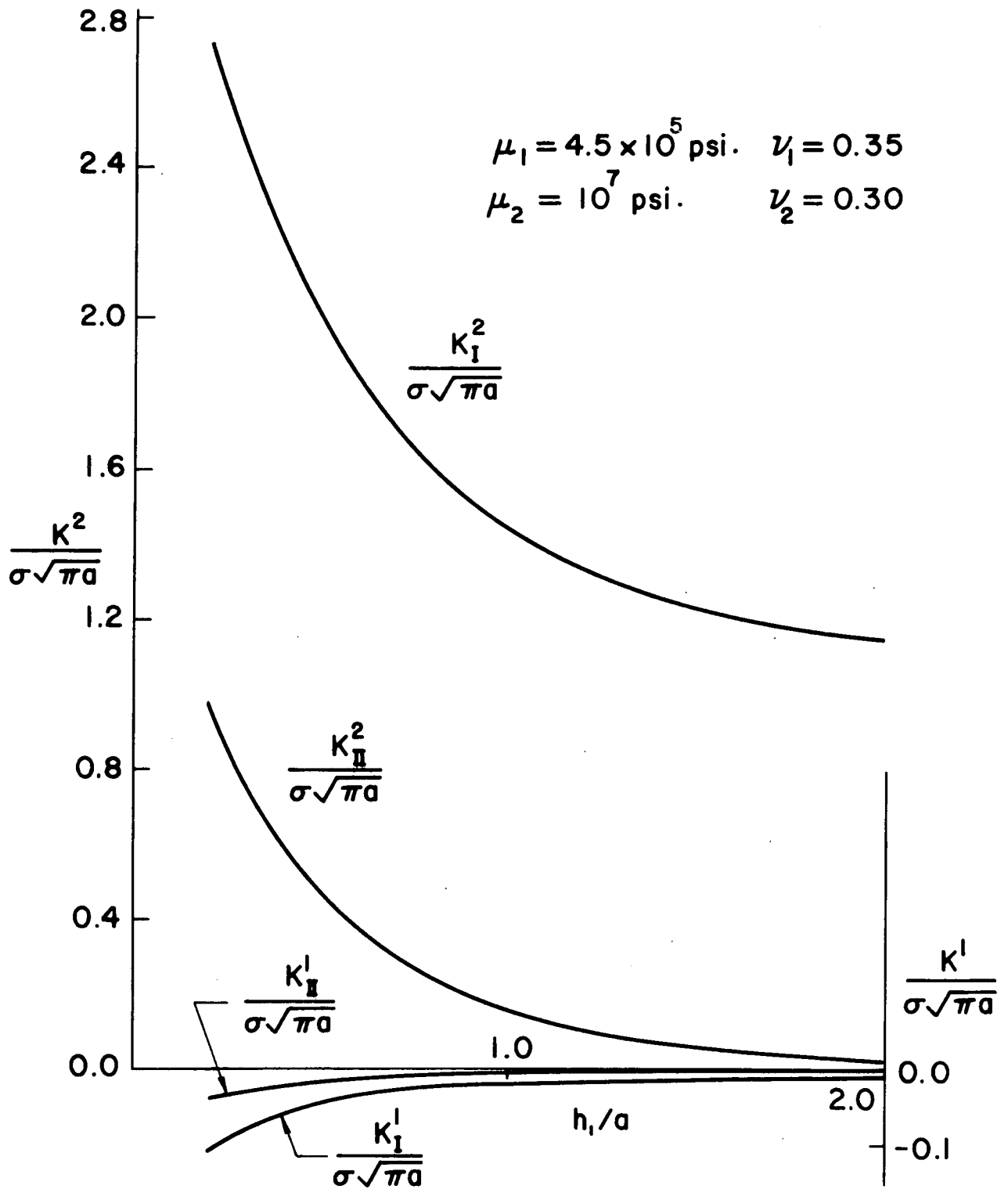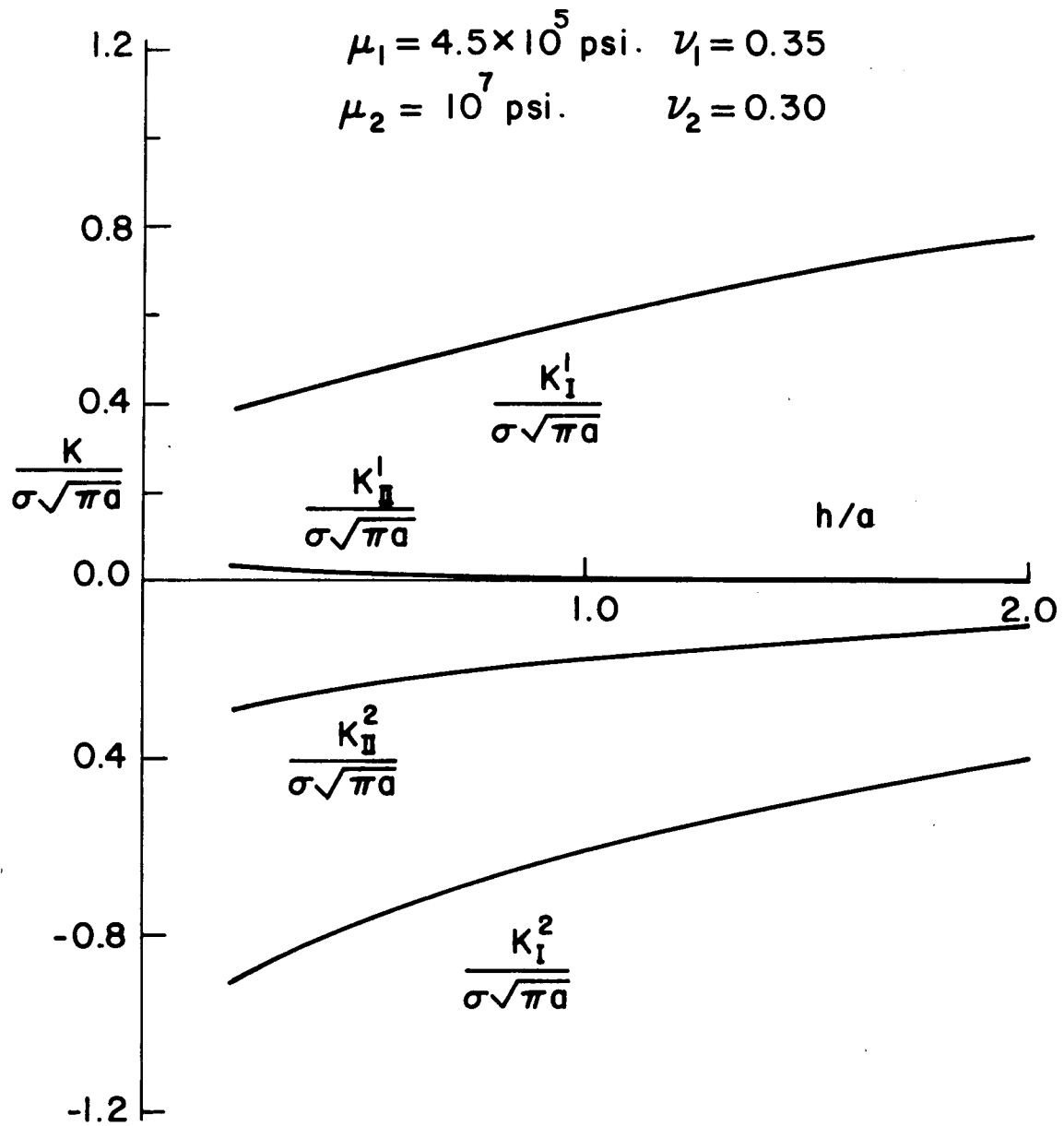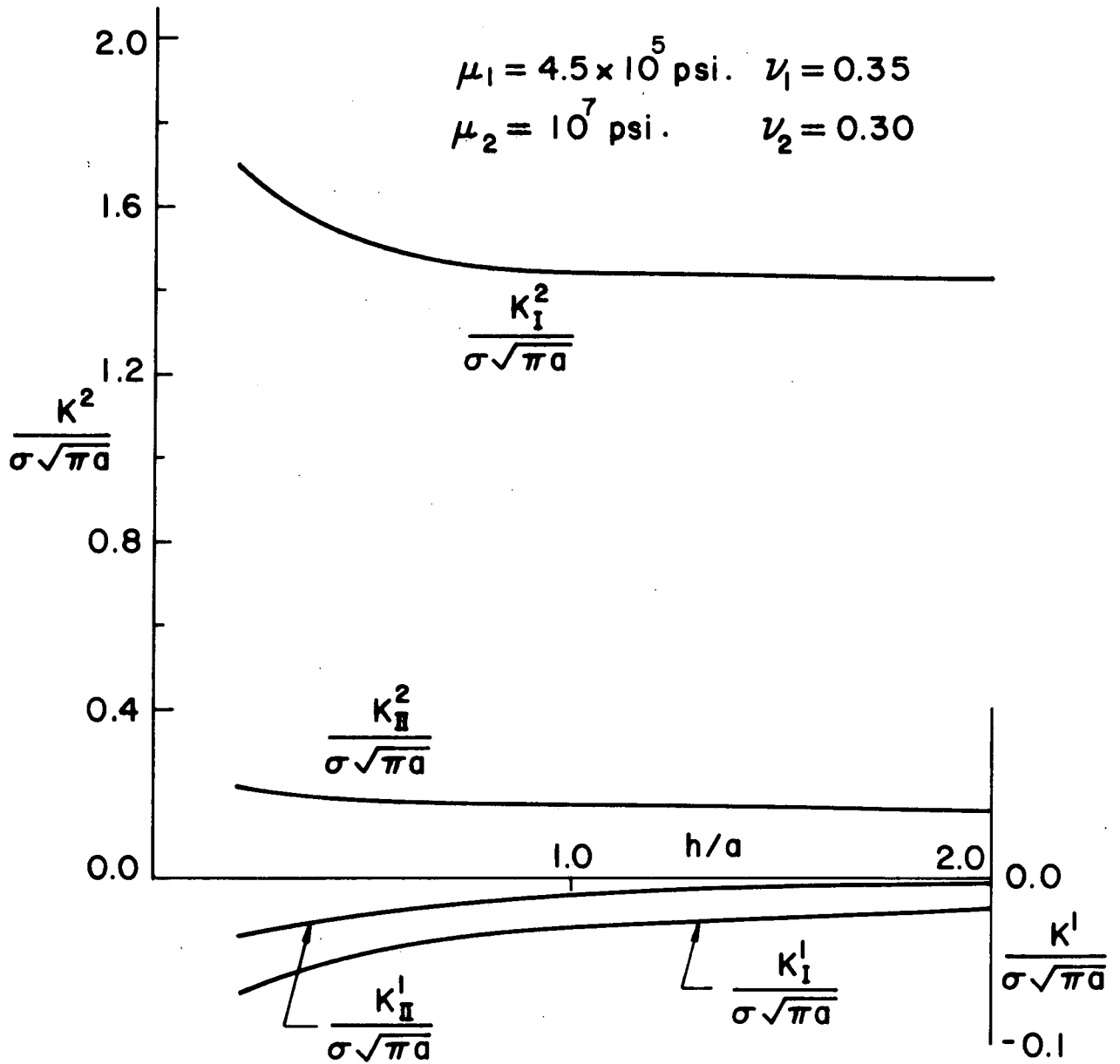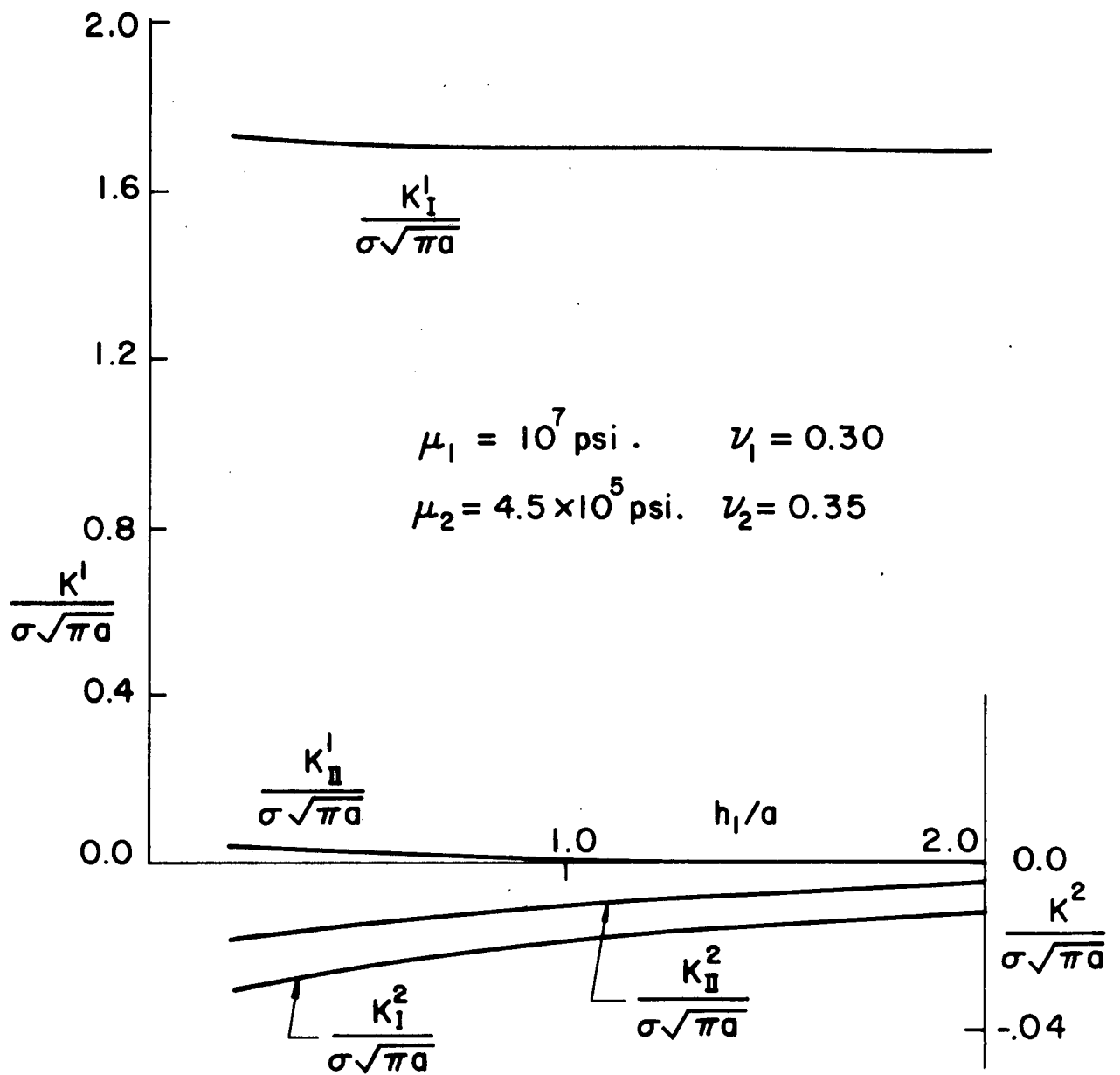
Figure 5. The Case with $q_2(x) = -\sigma$ and $p_1(x) = p_2(x) = q_1(x) = 0$.

Figure 6. Stress Intensity Factors vs. the Layer Thickness h/a for $h_1/a = 1.0$, $p_2(x) = -\sigma$ and $p_1(x) = p_2(x) = q_2(x) = 0$.

Figure 7. The Case with $q_2(x) = -\sigma$ and $p_1(x) = p_2(x) = q_1(x) = 0$.

Figure 8. Stress Intensity Factors vs. h_1/a for the Aluminum
Layer Sandwiched Between Epoxy Half-Planes.
h/a = 1.0, $p_2(x)$ = $-\sigma$ and $q_2(x)$ = 0.
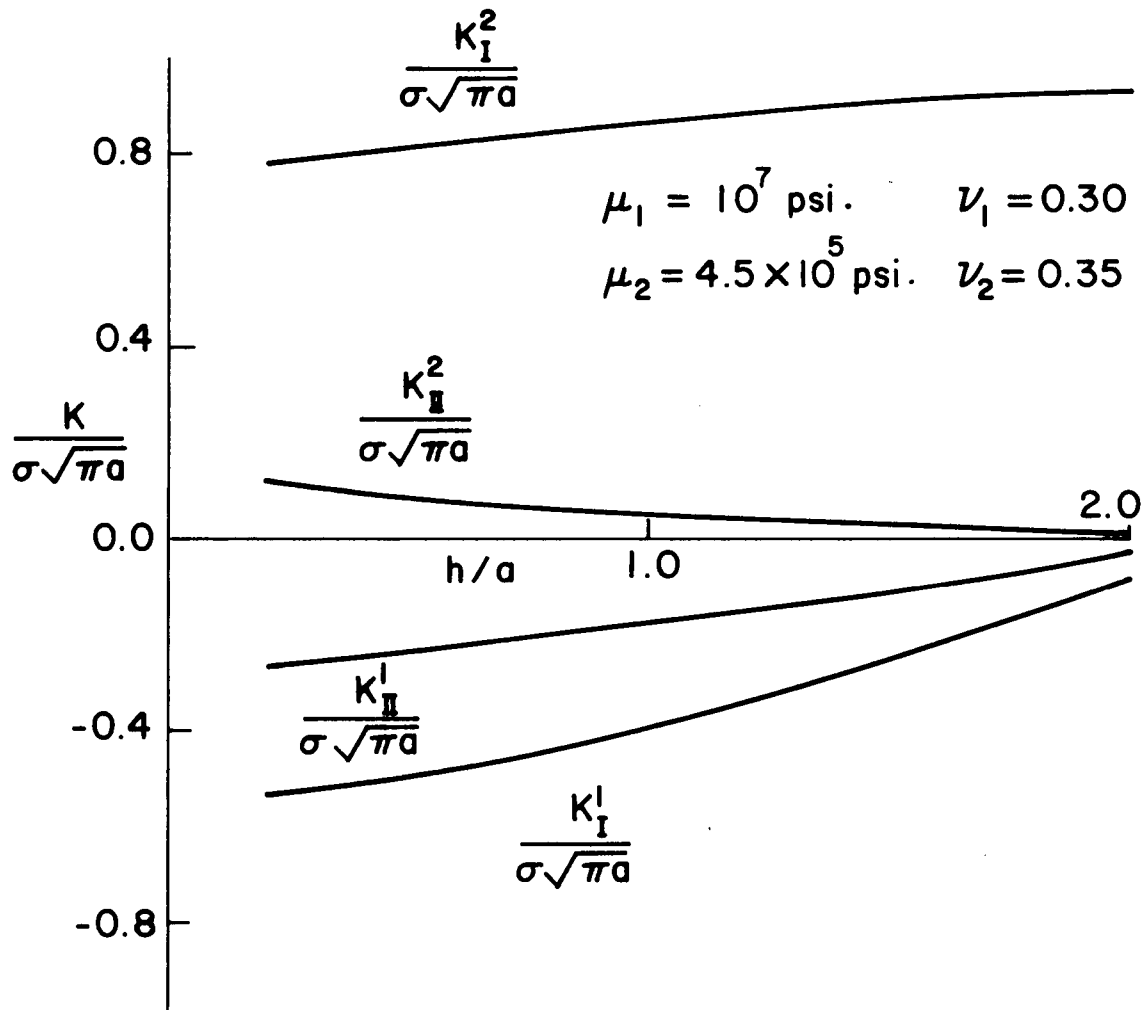
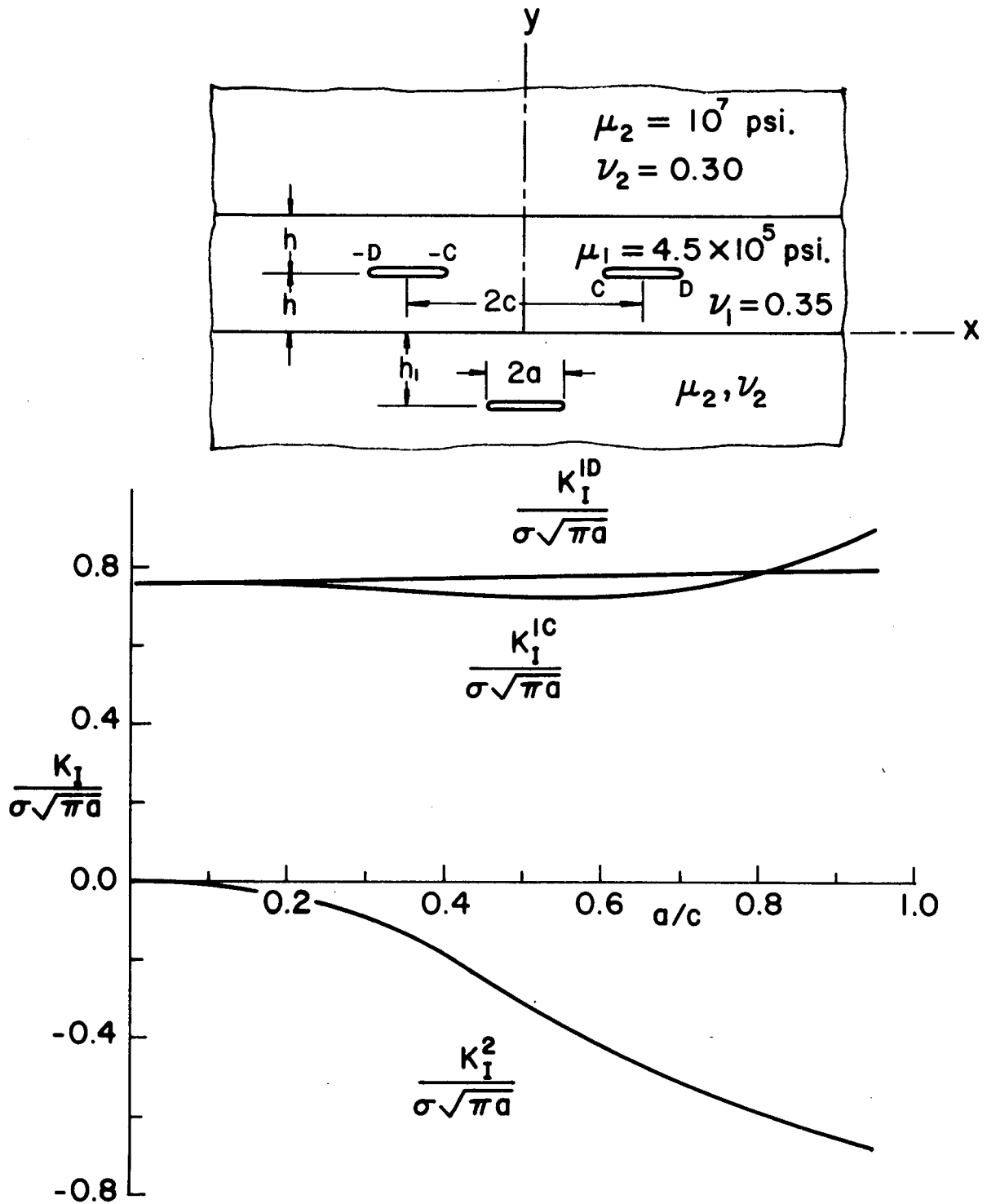Figure 9. Stress Intensity Factors vs. h/a; $h_1/a = 1.0$, $q_2(x) = -\sigma$ and $p_2(x) = 0$.

Figure 10. Stress Intensity Factor K_I vs. the Distance Between the Collinear Cracks (a/c). $p_2(x) = -\sigma$ and $q_2(x) = 0$.
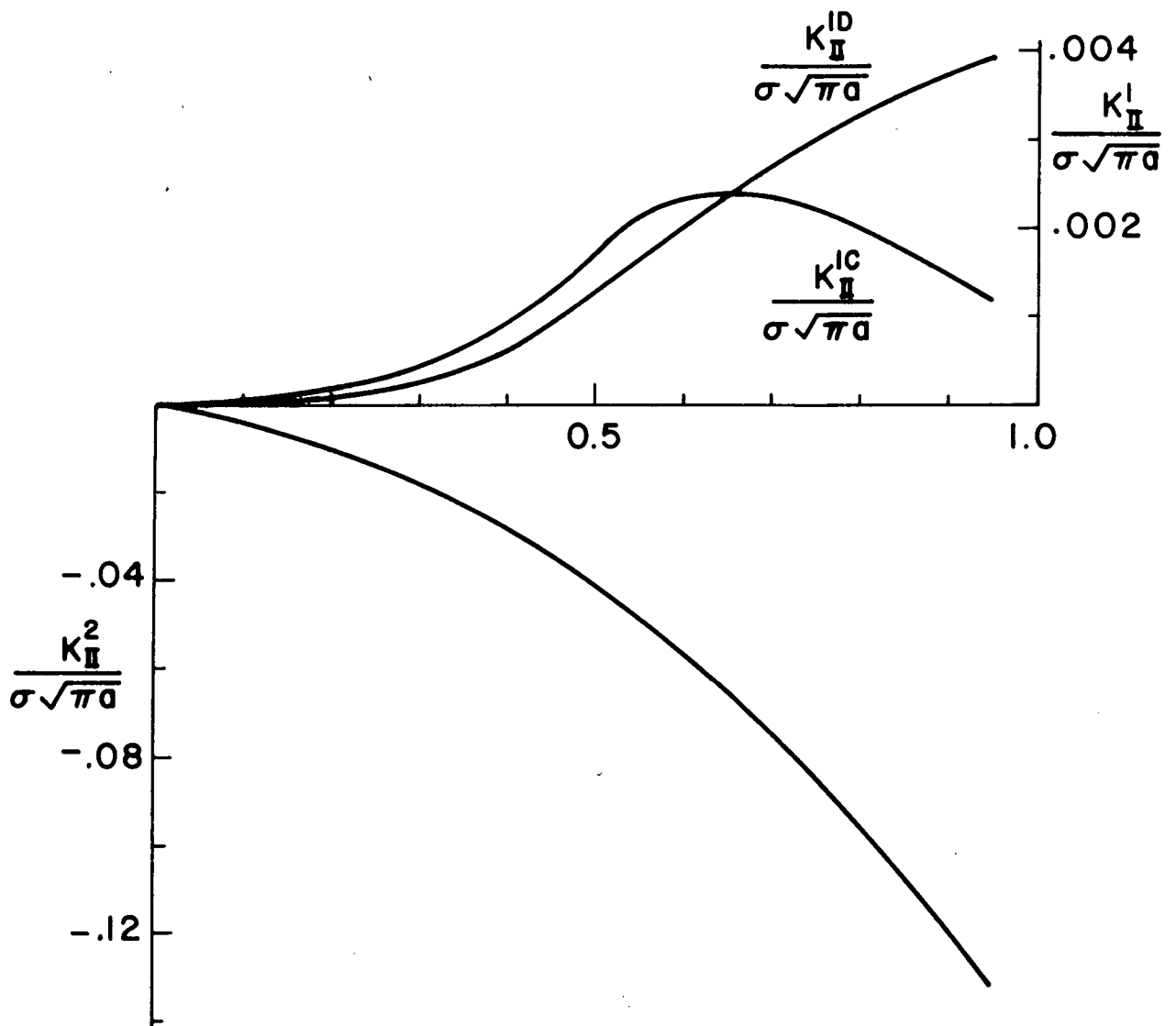
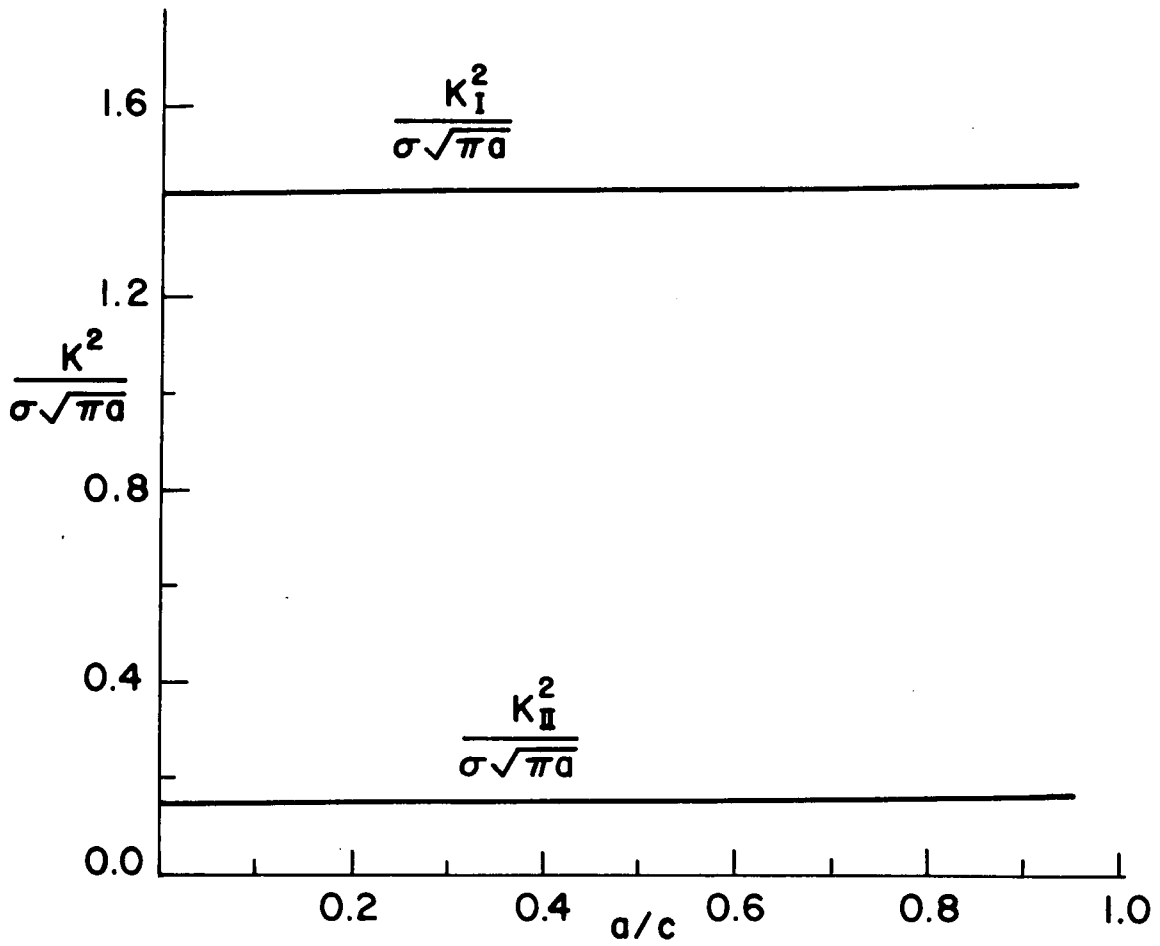Figure 11. K_{II} vs. a/c. $p_2(x) = -\sigma$ and $q_2(x) = 0$.

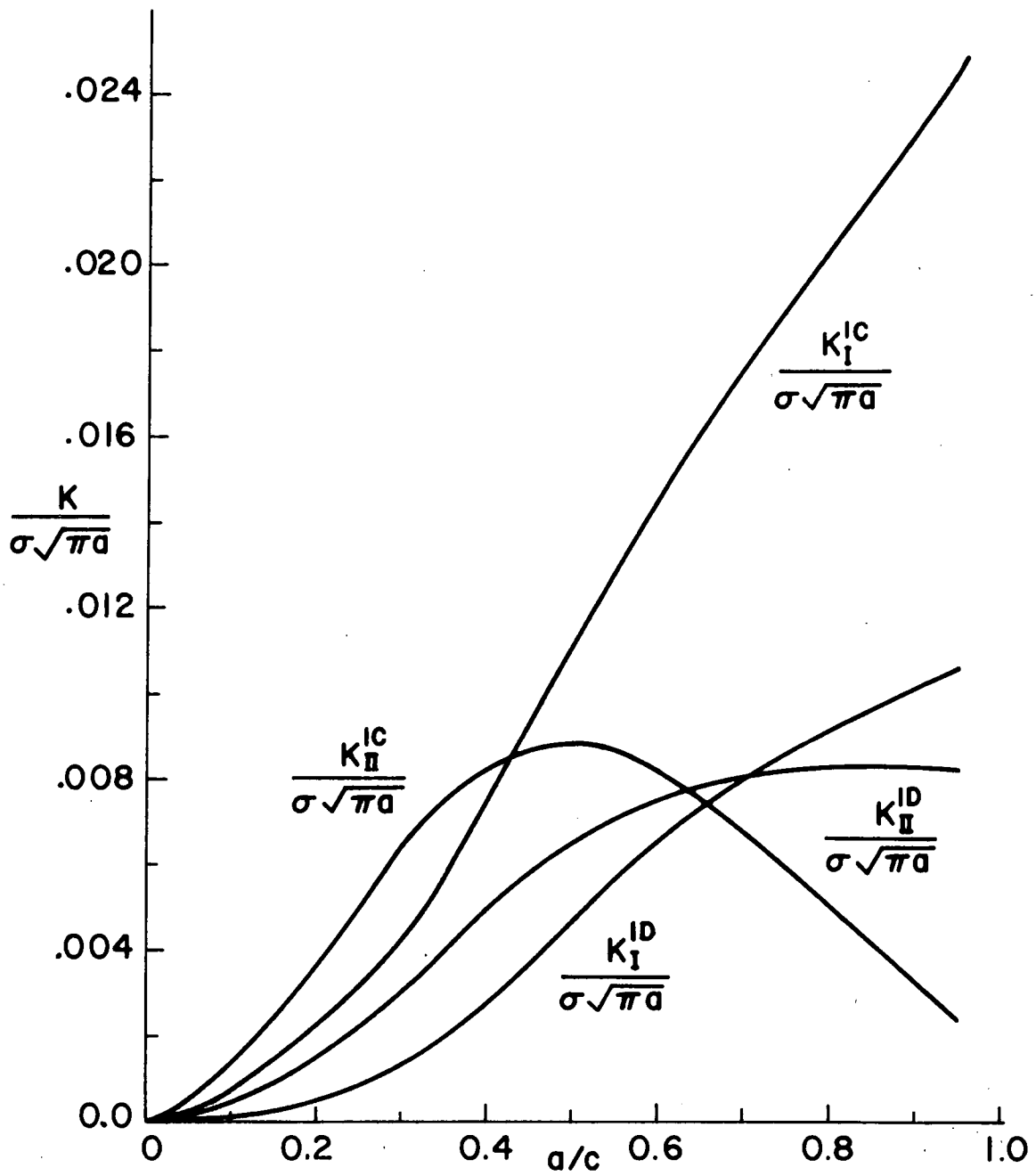Figure 12. K_I vs. a/c. $q_2(x) = -\sigma$ and $p_2(x) = 0$.

Figure 13. K_{II} vs. a/c. $q_2(x) = -\sigma$ and $p_2(x) = 0$.